Journal of Power Sources, 3 (1978) 81 - 94

EVALUATION AND OPTIMIZATION OF PELLETIZED LiAl/$NaAlCl_4$/$MoCl_5$ ELECTROCHEMICAL CELLS*

J. C. NARDI, J. K. ERBACHER, C. L. HUSSEY and L. A. KING

Frank J. Seiler Research Laboratory (Air Force Systems Command), U.S. Air Force Academy, Colorado 80840 (U.S.A.)

(Received November 16, 1977; in revised form February 2, 1978)

Summary

A proposed, low temperature molten salt thermally activated reserve battery (thermal battery) was investigated using single cell testing techniques. The basic electrochemical system utilized a lithium–aluminum alloy anode, a $MoCl_5$ cathode in intimate contact with a powdered graphite current collector, and an immobilized $AlCl_3$–NaCl electrolyte (m.p. 152 °C). This electrochemical system is a candidate to replace or complement existing thermal battery systems, all of which operate at much higher temperatures. Optimization of cells with respect to anode, electrolyte, and catholyte composition was investigated. Cell discharge behavior was characterized, defining optimum conditions of temperature and discharge rate to produce maximum available energy density.

Introduction

A thermal battery is a thermally activated reserve battery whose cells contain an electrolyte that is solid and non-conductive at normal temperatures but when melted becomes ionically conductive. A built-in pyrotechnic heat source activates the battery by melting the solid electrolyte. These characteristics make thermal batteries capable of essentially unlimited storage life and of rapid and reliable activation. Thermal batteries can be designed to withstand severe shock and vibrations, and, especially if pelletized construction is utilized, high spin rates. Therefore, they are able to fulfill certain military, aerospace, and emergency applications.

Thermal batteries are based on fused salt electrolyte systems. Investigations by various workers [1 - 8] have indicated relatively few electrochemical systems for thermal battery use which are capable of achieving high

*Paper presented at The International Symposium on Molten Electrolytes and High Temperature Batteries organized by the Electrochemistry Group of the Chemical Society, Brighton, Gt. Britain, September 22 - 23, 1977.

energy density output. Thermal batteries presently in production use either LiCl–KCl or LiBr–KBr electrolytes. They operate at high temperatures (400 - 600 °C), thereby incurring some obvious inherent disadvantages. The disadvantages of high temperature operation have led us to investigate a low temperature electrochemical system for use in high energy density thermal batteries.

Of the electrochemical systems having potential use in thermal batteries, aluminum chloride–alkali chloride mixtures are one of the few classes of inorganic molten salts that form relatively low melting compositions. Because they are also good ionic conductors [9], their use as battery electrolytes would lessen problems associated with the high operating temperatures of present molten salt electrolyte systems, while retaining the advantage of high energy density. The specific $AlCl_3$ electrolyte reported here is NaCl-saturated $AlCl_3$–NaCl, which has a specific conductivity of 0.4074 Ω^{-1} cm^{-1} at 175 °C [10] and a melting point of 152 °C. The apparent mole fraction of $AlCl_3$ in NaCl-saturated melt at 175 °C is 0.498 [11].

Early single cell studies in our laboratory of various anode–cathode couples in $AlCl_3$–NaCl electrolytes showed that the LiAl/$MoCl_5$ couple can be used to make a viable high energy density, high discharge rate cell [12]. Studies have been conducted on the preparation of molybdenum [13, 14] and the electrochemistry of several molybdenum salts [15, 16] in various electrolytes. There have been a few references to the use of molybdenum compounds in batteries [17 - 21], but no reported application of $MoCl_5$ to a thermal battery system.

It was our expectation that the single cell tests reported in the present work would be semi-quantitative indicators of multicell, *i.e.*, battery, performance.

Experimental

Inert atmosphere system

Electrolyte preparation, cell fabrication, and single cell discharge experiments were conducted in either a nitrogen or argon filled inert atmosphere system (Vacuum/Atmospheres Co. Model HE-43-6 Dri-Lab/HE-493 Dri-Train). The moisture content was maintained below 15 $p.p.m._V$ and the oxygen content was estimated to be 5 $p.p.m._V$ using the 25 W lightbulb method of Foust [22]. Initially all experiments were performed under a nitrogen atmosphere, but when lithium–aluminum alloys were used as anodes the atmosphere was converted to argon to preclude formation of lithium nitrides and the associated lithium fire hazard.

Electrolyte materials

Aluminum chloride

Puriss anhydrous iron free $AlCl_3$ was obtained from Fluka through Tridom Chemical Inc. and was used as received.

Sodium chloride

"Baker Analyzed" reagent grade NaCl was used as received.

Binding agent

Cab-O-Sil® (The Cabot Corporation), a high surface area fumed silicon dioxide, was obtained from the Cabot Corp. and was dried at 400 °C for one hour prior to use.

Cathode and anode materials

Molybdenum(V) chloride

Anhydrous 99.5% $MoCl_5$ was obtained from Research Organic/Inorganic Chemical Corp. in granular form. It was subsequently separated using standard ASTM sieves into <30, 30 - 50, 50 - 100, and >100 mesh sizes.

Graphite

Commercial graphites were obtained from Fisher Scientific Co. (Grade 38) and Superior Graphite Co. (No. 1 large graphite flakes). The Fisher graphite was used as received. The Superior graphite flakes were ground before use in a CRC Micro-Mill® (The Chemical Rubber Co.) and purified at 600 °C under a chlorine atmosphere [23].

Acetylene black

Acetylene black was obtained from Fisher Scientific Co. and used as received.

Aluminum

Powdered aluminum (99.9% pure, 100 mesh) was obtained from Research Organic/Inorganic Chemical Corp. and used as received.

Lithium–aluminum alloys

Lithium–aluminum alloys were obtained from Foote Mineral Co. (90.2 a/o lithium sheet and 60.2 and 48.0 a/o lithium powder) and stored under an argon atmosphere. The alloy powders were used as received. The alloy sheet was cut to 2.86 cm diameter circles prior to use.

Current collectors

Nickel foil 0.0127 cm thick was obtained from Alfa-Ventron, Inc. (99.98% pure). It was cut into 2.86 cm diameter circles with tab. The collectors were burnished with emery paper, washed with water and acetone, and again lightly burnished before use. The current collectors were used repeatedly throughout the single cell experiments and were cleaned prior to each use as just described.

Electrolyte preparation

Aluminum chloride was fused with excess NaCl at 175 °C and electrolytically purified for 24 hours utilizing a procedure developed by Boxall

et al. [24]. Ten w/o Cab-O-Sil was combined with the molten $NaCl-AlCl_3$ mixture to form a homogeneous paste. The resulting electrolyte–binder mixture (EBM) was cooled, ground to a powder with a CRC Micro-Mill, and stored under an inert atmosphere.

Pellet fabrication

Battery pellets were formed in a 2.86 cm diameter Carver die (Fred S. Carver, Inc.). Pellets made in this die had a facial surface area of 6.41 cm^2. The technique for casting a three-layer pellet was to spread the desired weight of metal powder evenly over the die surface and press at 1.17×10^7 kg/m^2. Next, a layer of EBM was added to the die and pressed at 1.62×10^7 kg/m^2. Finally, premixed cathode–graphite (with the addition of acetylene black in certain instances) –EBM was added and pressed at 2.05×10^7 kg/m^2. When sheet anodes were used, the first step cited above was omitted, and the EBM layer was pressed at 1.17×10^7 kg/m^2.

Individual component weights in pellets were known to ± 0.005 g. Any pellets for which the total weight differed from the sum of individual component weights by more than ± 1.0% were discarded.

The hydraulic press used to achieve these pressures was constructed from a 3.5×10^6 kg/m^2 hydraulic cylinder (Miller Fluid Power Division) having a 8.255 cm bore and a 25.4 cm stroke, and an Enerpac Model PER 2041 hydraulic pump (Applied Power, Inc.). The press was mounted through the glove box floor with the hydraulic cylinder, pump, and valves outside, while the head and platen of the press were inside. This type of mount prevented contamination of the atmosphere of the glove box with hydraulic fluid.

Single cell tests

Platen press

A platen press was used to hold the anode and cathode plates against the pellet during the cell test. The press was based on a design by Bush [25]. It consisted of two circular boron nitride platens approximately 3.3 cm in diameter and 2.54 cm thick, one of which was fixed and the other was attached to the piston of a Universal Midget pneumatic cylinder (Parker-Hannifin, Inc.), which had a 1.905 cm bore and a 5.08 cm stroke.

The platens were heated by means of two Thunderbolt TB-381, 120 V, 100 W cartridge heaters (Vulcan Electric, Inc.) in each platen wired in parallel and driven by an Electromax III Controller (Leeds and Northrup, Inc.) using a chromel–alumel thermocouple sensor. Temperature measurement was obtained from an ice/water referenced chromel–alumel thermocouple monitored with a DANA Model 5330/700 digital multimeter. The analog output from the multimeter was recorded graphically using an HP 7100B recorder (Hewlett Packard Inc.). Each platen could be heated from room temperature to a stable 175 °C in three minutes and be controlled at the desired discharge temperature to ± 0.3 °C. Overall temperature control during a single cell discharge experiment was ± 0.5 °C.

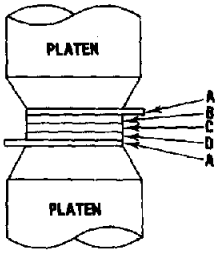

Fig. 1. Single cell test setup. A, current collectors; B, anode; C, electrolyte; D, catholyte.

A three-layer cell placed between platens is shown schematically in Fig. 1.

Pressure on the single cells during test was maintained at 3200 kg/m^2 using high purity argon from the same tank that supplied the inert atmosphere system.

Cell discharge

The single cells were clamped in the platen press, the platens were heated to the desired temperature, and cell discharge was initiated when the cell voltage had stabilized.

Constant current discharge was maintained by a PAR Model 371 potentiostat/galvanostat (Princeton Applied Research Corp.) and the current was quantitatively measured with a PAR Model 379 digital coulometer. Cell voltage was recorded on an HP 7100B recorder. An additional set of leads was connected across the single cell which allowed the cell voltage to be sampled by a DEC PDP 11/10C data acquisition system. Data were taken at the smallest convenient equally spaced increments of time. Subsequent data reduction was done with the aid of the computer.

Results and discussion

It was evident from the analysis of single cell discharge data that varying the anode, electrolyte, and catholyte compositions had significant effects on overall output and cell efficiency. The criterion used for ranking the "goodness" of single cell performance was the experimental energy density based on the total mass of the cell pellet:

$$\text{Energy density} = \frac{iEt}{m}$$

where

$$Et = \int_0^{t(E=0)} E\,dt \simeq \sum_{t=0}^{t(E=0)} \frac{E_t + E_{t+\Delta t}}{2}\,\Delta t$$

It should be noted that calculations were based upon discharge to 0.0 V rather than to some defined percentage of initial voltage cut-off which one might expect for useful battery performance. This was done primarily because of an ambiguity in defining initial voltage, as will be seen below in the description of anode behavior.

The composition of our best single cells is given in Table 1. Variables which were considered in the cell optimization study were anode composition, anode weight, separator electrolyte weight, catholyte electrolyte weight, $MoCl_5$ particle size, and graphite weight. The effects of these parameters on cell performance are noted in Tables 2 - 8. Table 9 gives specific descriptions of the cell configurations. The composition of the electrolyte itself and the amount of Cab-O-Sil binder present are not necessarily optimum values, but our experience has shown them to be well suited for studying a variety of thermally activated single cells, including at least 40 cathode materials [12, 23, 26, 27].

The maximum expected uncertainty in a given weight ratio was ± 3%, as calculated from the uncertainties in individual component and total pellet weights. The uncertainty in platen press pressures was ± 5%; however, there are no data on the influence of platen press pressure on cell performance. Bush [25] states that thermal cells with LiCl–KCl electrolytes behave independently of platen press pressure at pressures above 1230 kg/m^2. We used 3200 kg/m^2.

TABLE 1

Optimized cell component configuration

Section	Weight (g)[a]	Component
Anode	0.27	60.2 a/o Li–LiAl alloy
Separator	0.78	EBM[b]
Cathode	0.64	EBM[b]
	0.72	$MoCl_5$ (30 - 50 mesh)
	0.23	Graphite (Fisher)

[a]For 2.86 cm diameter cells

[b]EBM: 90 w/o electrolyte (49.85 m/o $AlCl_3$–50.15 m/o NaCl) plus 10 w/o Cab-O-Sil.

TABLE 2

Optimization of LiAl composition

Li a/o in LiAl alloy	Energy density (Wh/kg)
48.0	76.3
60.2	81.6
90.9	73.9

TABLE 3

Optimization of anode weight

Anode weight (g)	Energy density (Wh/kg)
0.27	60.8
0.29	58.0
0.34	48.9
0.43	43.7

TABLE 4

Optimization of separating EBM weight

Electrolyte weight (g)	Energy density (Wh/kg)
0.74	67.5
0.78	69.2
0.82	60.8
0.99	26.2

TABLE 5

Optimization of EBM weight in cathode region

$NaAlCl_4$ weight (g)	Energy density (Wh/kg)
0.51	60.0
0.58	46.5
0.64	69.2
0.77	53.1
0.90	49.4

TABLE 6

Optimization of $MoCl_5$ particle size

Particle size (ASTM mesh)	Energy density (Wh/kg)
<30	53.4
30 - 50	48.9
50 - 100	38.4
>100	37.3

TABLE 7

Optimization of $MoCl_5$ weight

$MoCl_5$ (30 - 50 mesh) weight (g)	Energy density (Wh/kg)
0.52	63.3
0.72	69.2
0.79	69.0
0.86	61.3
0.94	71.9
1.00	67.0

TABLE 8

Optimization of graphite weight

Graphite weight (g)	Energy density (Wh/kg)
0.18	64.2
0.21	62.2
0.23	69.2
0.25	64.8
0.27	62.6

Anodes prepared from pure aluminum and from 48.0, 60.2, and 90.9 a/o Li in LiAl alloys were tested. The aluminum anode performed much more poorly than did any of the LiAl alloys (Fig. 2). We have found this to be a general pattern in other instances as well [12, 26]. This may be the result of surface oxide, but we have made no effort to circumvent this behavior. Pure lithium anodes were also studied, and these also performed poorly. Moreover, the low melting point of lithium metal effectively precludes its use in thermal batteries. The three alloys examined performed similarly (Table 2), with a noticeable advantage displayed by the 60.2 a/o alloy.

TABLE 9

Cell optimization data

Variable being tested[a]	Table No.	Anode[b] weight (g)	EBM[c] separator weight (g)	Cathode weights (g)		
				EBM[c]	$MoCl_5$[d]	Graphite[e]
Anode composition	2	0.27	0.78	0.64	0.72	0.23
Anode weight	3	–	0.82	0.64	0.72	0.23
Separating EBM weight	4	0.27	–	0.64	0.72	0.23
Catholyte EBM weight	5	0.27	0.78	–	0.72	0.23
$MoCl_5$ particle size	6	0.34	0.82	0.64	0.72	0.23
$MoCl_5$ weight	7	0.27	0.78	0.64	–	0.23
Graphite weight	8	0.27	0.78	0.64	0.72	–

[a] All except Table 2 at 15 mA/cm^2. Table 2 at 25 mA/cm^2. All at 200 °C.
[b] All 60.2 a/o Li LiAl alloy except Table 2.
[c] EBM: 90 w/o electrolyte (49.85 m/o $AlCl_3$–50.15 m/o NaCl) plus 10 w/o Cab-O-Sil.
[d] All ASTM 30 - 50 mesh except Table 6.
[e] Fisher.

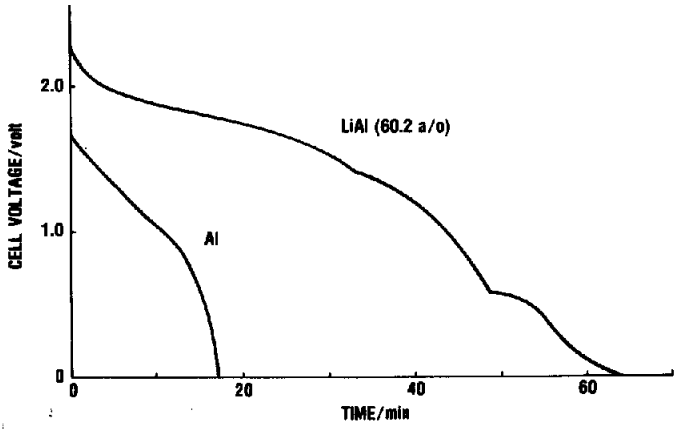

Fig. 2. Discharge curves of single cells utilizing Al or LiAl alloy anodes (25 mA/cm^2 at 175 °C).

Unfortunately, cells utilizing LiAl alloy anodes always exhibited a high-voltage "spike" during activation. Pure aluminum anodes did not exhibit this behavior. The spike typically reached about 3.7 V and occurred as the electrolyte approached its melting temperature, whereupon cell voltage immediately decayed to an open circuit voltage characteristic of pure aluminum anodes at the same electrolyte temperature. The presence of a sharp spike correlated positively with good quality single cell performance. Voltage spiking also has been observed with pure lithium anodes [26] and with a lithium–boron alloy anode (supplied courtesy of the Naval Surface Weapons Center, White Oak Laboratory, Electrochemistry Division, Silver Spring, MD).

In fact, the behavior of pure lithium anodes was indistinguishable f. .n LiAl alloys in the voltage spike region of cell activation/discharge. Similar behavior was observed by Ryan and Bricker [28] and Marsh *et al.* [29] for thermal batteries, where a load was applied during and after activation, although of course voltages were not the open circuit values. As noted in the latter two references, any voltage irregularities are very undesirable in an operating battery, and an investigation of this behavior and its dependence on alloy composition is underway in our laboratory.

These results suggest that lithium is the active anode material in the presence of unmelted electrolyte, and that lithium reacts with molten electrolyte to produce aluminum, which is then the active anode [26].

Table 3 shows that energy density increased as the anode weight decreased. However, pellets containing less than 0.27 g of alloy would disintegrate when physically handled in assembling test cells.

The effect of the $MoCl_5$ particle size on overall performance (Table 6 and Fig. 3) shows that the highest energy density was obtained with the larger particle size. However, the use of this size resulted in a crumbly catholyte layer with ragged edges. The 30 - 50 mesh $MoCl_5$ particles were used to insure uniform pellet construction. The improved performance by cells with the larger $MoCl_5$ particle size could be explained assuming that the larger, lower surface area particles dissolve at a slower rate in the electrolyte, and thus diffusional transport to the anode resulting in internal parasitic current is lessened. An obvious test of this assumption would be to evaluate the dependence of cell performance upon $MoCl_5$ particle size as a function of constant current discharge rate. Such a study has not been performed.

The weight optimizations listed in Tables 4, 5, 7, and 8 are self-explanatory. The addition of 1% of total pellet weight of acetylene black to the catholyte increased cell energy density very slightly, but consistently.

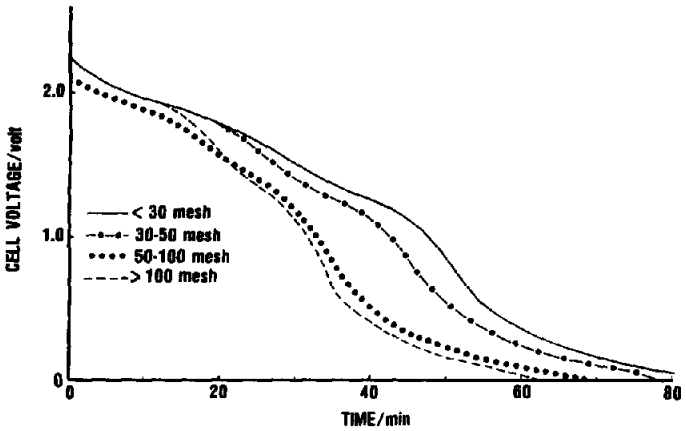

Fig. 3. Effect of $MoCl_5$ particle size on single cell discharge (15 mA/cm^2 at 175 °C).

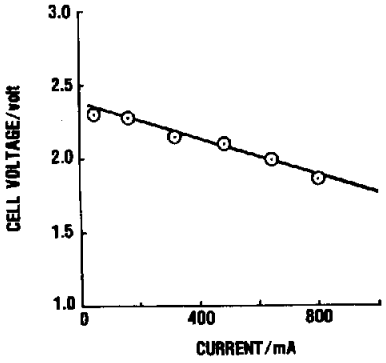

Fig. 4. Single cell internal resistance determination.

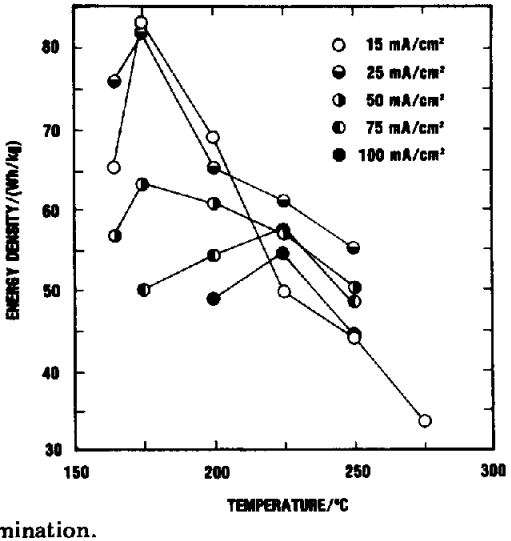

Fig. 5. Dependence of energy density upon temperature and discharge rate.

This observation suggests the possibility of a further optimization of current collection within the catholyte volume.

The internal resistance of cells of optimized configuration (Table 1) was determined by measuring cell voltage under load as varying loads were imposed on a series of cells. Cell resistance calculated from the data shown in Fig. 4 was 0.63 Ω.

Discharge behavior of single cells of the composition specified in Table 1 was also investigated as it depended on temperature and discharge rate. Constant current discharges of 15, 25, 50, 75, and 100 mA/cm^2 were made at temperatures of 165, 175, 200, 225, and 250 °C. The results are shown in Fig. 5. A sharp drop in energy density was noted at temperatures above the melting point of $MoCl_5$ (194.5 °C). This may be due to an increased rate of transport of Mo(V) to the anode at temperatures above the melting point of $MoCl_5$, a possibility further suggested by the observation that peak performance occurred at higher currents at higher temperatures.

The highest observed energy density of 83.3 Wh/kg was achieved at 175 °C and a discharge rate of 15 mA/cm^2. (Cell thicknesses were not recorded, however, this energy density corresponds to a volumetric energy density of approximately 0.3 - 0.4 Wh/cm^3.) The maximum available energy density based on an overall five electron reduction at the open circuit voltage of molybdenum at the cathode is 420 Wh/kg, which indicates an optimized single cell efficiency of 20%. The total charge available from the lithium and the aluminum in 0.27 g of 60.2 a/o Li LiAl alloy and 0.72 g of $MoCl_5$ is 1050, 2090, and 1270 C, respectively. The "best" cell cited above produced 616 C. The coulombic efficiency based on lithium, aluminum and $MoCl_5$ was 59%, 29%, and 49%, respectively.

At a discharge rate of 25 mA/cm^2, the calculated energy density decreased to 81.6 Wh/kg. The marked decrease in energy density at even higher discharge rates may be due to diffusional limitations, and in addition, slow interposed chemical steps in the cathode reduction mechanism. Mo(V) has been shown to be reduced to Mo(III) at the diffusion rate in basic (NaCl-rich) melts. However, chemical steps and other kinetic complications appear during further reduction [16]. The reduction of Mo(V) has not been thoroughly investigated in neutral or acid ($AlCl_3$-rich) $AlCl_3$–NaCl melts.

Figures 2 and 3 demonstrate that the overall discharge process is complex. We used a method proposed by Balewski and Brenet [30] to examine the cell discharge mechanism. This use of the derivative of the discharge curve is the first application of the method to thermal battery analysis. The influences of variations in operating temperature and type of graphite in the catholyte were studied for the optimum cell (Table 1) at 15 mA/cm^2. The slope and average voltage were calculated at 100 s intervals.

Figure 6a shows the derivative plot for a single cell discharge at 175 °C utilizing Fisher graphite in the catholyte. The major peak was centered at

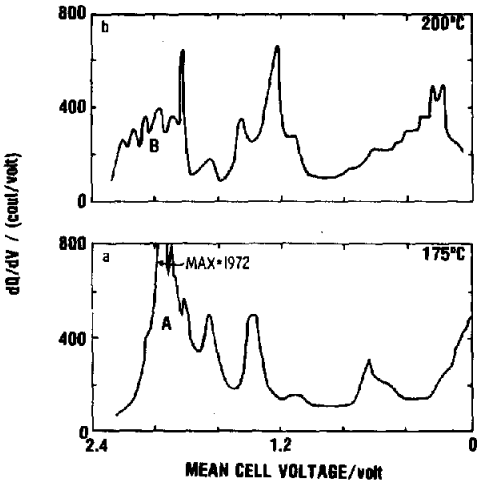

Fig. 6. Derivative of the discharge curve using unpurified Fisher graphite (15 mA/cm^2, 100 s intervals). (a) 175 °C; (b) 200 °C.

1.91 V. Comparison of the derivative plots at 175 °C and at 200 °C (Fig. 6b) shows that prominence of the peaks shifts to lower voltage at the higher temperature. This tendency is even more pronounced at 250 °C (not shown).

A comparison of the areas under the individual peaks shows that as the operating temperature is increased the major supporting reactions occur at lower potentials. For example, the discharge step represented by peak A contributed approximately 38% of the total charge delivered at 175 °C. This percentage decreased to 29% at 200 °C (peak B) and finally to 22% at 250 °C. Only 27% of the total coulombs were supplied below 0.8 V by the single cell

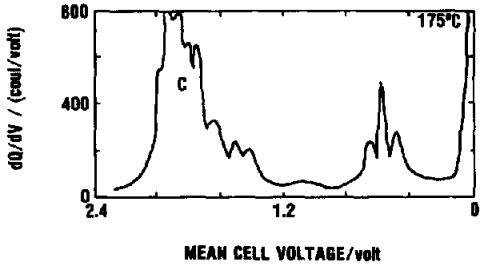

Fig. 7. Derivative of the discharge curve using purified Superior graphite (15 mA/cm^2, 100 s intervals, 175 °C).

discharged at 175 °C. This value successively increased to 40% and 54% at temperatures of 200 °C and 250 °C respectively. In an operational battery configuration, voltage constraints often require voltage cutoffs to be 80% of initial closed circuit voltage. If one were to apply this criterion to single cell experiments, this would indicate an optimized single cell operating temperature of 175 °C.

The derivative plots for the optimized single cell utilizing the purified Superior graphite indicate that a change in operating temperature had little effect on the general shape of the curves. The derivative plot at 175 °C (Fig. 7) shows that only three major peaks support the total discharge. The main reaction represented by peak C at 1.91 V contributed 54.7% of the total charge delivered, with reactions represented by the next two major peaks delivering 16.4% and 28.9% of the total output respectively. At successively higher temperatures a shift to lower voltage of peak prominence was again noted. Furthermore, at all three temperatures, the purified Superior graphite discharge curve derivatives were smoother than were the results obtained from unpurified Fisher graphite. The three major peaks observed with purified Superior graphite are consistent with the suggestion of Phillips and Osteryoung [16] of a three-step reduction of Mo(V) to Mo(0) in tetrachloroaluminate melts.

Substitution of purified Superior graphite for unpurified Fisher graphite in an otherwise optimized single cell reduced the total coulombic output by 19% at 15 mA/cm^2 and 175 °C. In a similar study with LiAl/$NaAlCl_4$/$CuCl_2$ single cells [26] which were discharged to 1.0 V at 3.95 mA/cm^2 at 175 °C, the energy density for purified Superior, unpurified Fisher, and unpurified Superior graphites was 27.2, 30.2, and 31.9 Wh/kg, respectively. Substantial amounts of iron were shown by Brabson *et al.* [23] to be present in unpurified Superior graphite. In the latter study approximately 95% of the iron was removed in the same purification process that was used in the present work and in the $CuCl_2$ study [26].

We also have shown [27] that $FeCl_3$ is a suitable cathode material in its own right. In fact, at high temperature LiAl/$NaAlCl_4$/$FeCl_3$ single cells outperform LiAl/$NaAlCl_4$/$MoCl_5$ single cells (15 mA/cm^2 and 250 °C to 80% of initial closed circuit voltage).

These results suggest that the impurities which are present at least in the Fisher and Superior graphites we used are desirable, and in fact contribute substantially to the cell energy density.

Acknowledgements

We wish to express our appreciation to Professor R. A. Osteryoung of Colorado State University, Fort Collins, Colorado; and to D. M. Bush and B. H. Van Domelen at Sandia Laboratories, Albuquerque, New Mexico, for their helpful discussions. We also thank R. Hudson (Eagle-Picher Industries, Inc.) and G. Overall (Foote Mineral Co.) for contributing samples of several LiAl alloys.

References

1 S. M. Selis, L. P. McGinnis, E. S. McKee and J. T. Smith, J. Electrochem. Soc., 110 (1963) 469.
2 S. M. Selis, J. P. Wondowski and R. F. Justus, J. Electrochem. Soc., 111 (1964) 6.
3 H. Goldsmith and J. T. Smith, Electrochem. Technol., 6 (1968) 16.
4 L. H. Thaller, J. Electrochem. Soc., 115 (1968) 116.
5 B. H. Van Domelen and R. D. Wehrle, in 9th Intersociety Energy Conversion Engineering Conference Proceedings, American Society of Mechanical Engineers, New York, 1974, pp. 665 - 670.
6 F. Tepper, in 9th Intersociety Energy Conversion Engineering Conference Proceedings, American Society of Mechanical Engineers, New York, 1974, pp. 671 - 677.
7 G. C. Bowser, D. Harney and F. Tepper, in D. H. Collins (ed.), Power Sources 6, Academic Press, London, 1977, pp. 537 - 547.
8 C. W. Jennings, in N. C. Cahoon and G. W. Heise (eds.), The Primary Battery, Vol. Two, John Wiley, New York, 1976, pp. 263 - 293.
9 R. H. Moss, PhD Thesis, University of Connecticut, 1955.
10 R. C. Howie and D. W. Macmillan, J. Inorg. Nucl. Chem., 33 (1971) 3681.
11 G. Torsi and G. Mamantov, Inorg. Chem., 10 (1971) 1900.
12 C. L. Hussey, J. K. Erbacher and L. A. King, FJSRL Technical Report 76-0003, F. J. Seiler Research Laboratory, 1976.
13 S. Senderoff and A. Brenner, J. Electrochem. Soc., 101 (1954) 16.
14 E. E. Marshall and L. F. Yntema, J. Phys. Chem., 46 (1942) 353.
15 T. Suzuki, Electrochim. Acta, 15 (1970) 127.
16 J. Phillips and R. A. Osteryoung, J. Electrochem. Soc., 124 (1977) 1465.
17 L. Campanella and G. Pistoia, J. Electrochem. Soc., 118 (1971) 1905.
18 L. Campanella and G. Pistoia, J. Electrochem. Soc., 120 (1973) 383.
19 F. W. Dampier, J. Electrochem. Soc., 121 (1974) 656.
20 B. DiPietro, V. Filippeschi, M. Lazzari, G. Pistoia and B. Scrosati, in D. H. Collins (ed.), Power Sources 6, Academic Press, London, 1977, pp. 527 - 536.
21 T. Valånd, J. Power Sources, 1 (1976) 65.
22 R. A. Foust, Jr., Drybox Purity Control Using Exposed Light Bulb Filament, General Motors Technical Center Letter, Warren, MI, October 3, 1968.
23 G. D. Brabson, J. K. Erbacher, L. A. King and D. W. Seegmiller, FJSRL Technical Report 76-0002, F. J. Seiler Research Laboratory, 1976.
24 L. G. Boxall, H. L. Jones and R. A. Osteryoung, J. Electrochem. Soc., 121 (1974) 212.

25 D. M. Bush, in Proc. Twenty-Sixth Power Sources Symposium, PSC Publication Committee, Red Bank, NJ, 1974, pp. 144 - 147.
26 J. K. Erbacher, C. L. Hussey and L. A. King, FJSRL Technical Report 77-0001, F. J. Seiler Research Laboratory, 1977.
27 J. C. Nardi, J. K. Erbacher and C. L. Hussey, FJSRL Technical Report 77-0004, F. J. Seiler Research Laboratory, 1977.
28 D. M. Ryan and L. C. Bricker, Contract Report AFAPL-TR-77-12, Eureka Advance Science Corp., 1977.
29 R. A. Marsh, D. M. Ryan and J. C. Nardi, J. Power Sources, 3 (1978) 95.
30 L. Balewski and J. P. Brenet, Electrochem. Technol., 5 (1967) 527.